JOURNAL OF MATERIALS SCIENCE 33 (1998) 235–239

Amorphization behaviour in mechanically alloyed Ni–Ta powders

PEE-YEW LEE
Institute of Materials Engineering, National Taiwan Ocean University, Keelung, Taiwan 202
JU-LUNG YANG
Materials Research Laboratories, Industrial Technology Research Institute, Chutung, Taiwan 310
HONG-MING LIN
Department of Materials Engineering, Tatung Institute of Technology, Taipei, Taiwan 104

Amorphization behaviour of Ni_xTa_{100-x} alloy powders synthesized by mechanical alloying mixtures of pure crystalline Ni and Ta powders with a Spex high energy ball mill was studied. The mechanically alloyed powders were amorphous for the composition range between $Ni_{10}Ta_{90}$ and $Ni_{80}Ta_{20}$. This range is larger than amorphous alloys prepared by the rapid-quenching process or by electron-gun deposition technique. A supersaturated nickel solid solution formed for Ni-rich composition. The thermal stability has been investigated by differential thermal analysis. The crystallization temperature of amorphous Ni–Ta powders was proportional to the Ta content, and the activation energy of amorphous Ni–Ta powders exhibited a maximum near the eutectic composition. It is found that the amorphization rate at the early stage of the mechanical alloying process was faster in the intermediate compositions than those at both Ni- and Ta-rich compositions.

1. Introduction

The preparation of amorphous alloys based on IVa–VIa group transition metals, i.e., refractory transition metals, are very attractive because it is expected that amorphous phases of these high-melting-temperature alloys would possess high crystallization temperatures [1]. However, the high cooling rate required to bypass the nucleation and growth of more stable crystalline phases in the undercooled alloy melts always places a severe restriction on the process, particularly on the amorphization of alloy with a high melting temperature by the liquid quenching method [2]. Recently, it has been demonstrated that amorphous materials can also be obtained by destabilizing the crystallinity of a solid phase by solid-state reaction [3, 4]. Two general methods have been developed for synthesizing amorphous alloys based on a solid-state reaction: (i) amorphization by a solid-state interdiffusion process: (ii) amorphization by mechanical alloying (MA) [5].

MA was developed in the early 1970s mainly for the production of oxide-dispersion-strengthened superalloy powder [6]. It is a high-energy ball-milling process consisting of repeated mechanical mixing, cold welding, fracturing and rewelding of ultrafine alloy powder during ball–powder collision events [7]. By virtue of this special milling behaviour MA allows materials scientists to circumvent material limitations and to manufacture alloys that are difficult or impossible to produce by conventional melting and casting techniques. This process has generated great interest since the discovery of the amorphous phase in mechanically alloyed $Ni_{60}Nb_{40}$ powder by Koch *et al.* [8] in 1983. During the last decade, many equilibrium and/or non-equilibrium phases in a number of alloy systems have been successfully synthesized by means of this technique. These materials include amorphous alloys, nanocrystalline materials, quasicrystals, rare-earth magnets and intermetallics [9]. However, a survey of the available literature indicates that little work has been performed on the amorphization of Ni–Ta binary alloy by MA of elemental Ni and Ta powders. Therefore, the objective of the present research was to investigate the feasibility of preparing amorphous Ni–Ta powders by MA of elemental Ni and Ta powders using a shaker ball mill.

2. Experimental procedure

Elemental powders of Ni (purity 99.98%; less than 300 mesh) and Ta (purity, 99.98%; less than 325 mesh) were accurately weighed to give the desired compositions Ni_xTa_{100-x} ($x = 10, 20, 30, 40, 50, 60, 70, 80$ and 90). The pre-weighed powder mixtures were canned into an SKH9 high-speed steel vial together with Cr steel balls (7 mm in diameter) under an argon atmosphere within a glove-box. The ball-to-powder weight ratio was 2 to 1. A Spex 8000 shaker ball mill was employed for the MA process. The mill was installed inside an Ar-filled glove-box in order to control the

0022–2461

milling atmosphere. An oxygen analyser was also used to detect the oxygen content of the glove-box. The MA process was initiated when the analyser indicated that the oxygen content was undetectable. The process was interrupted every 30 min, followed by an equal length of time to cool the vials, which had been heated up typically to about 50 °C. A suitable quantity of the mechanically alloyed powders was taken out of the steel vial periodically to observe the progress of alloying by X-ray diffraction and scanning electron microscopy (SEM) techniques. The X-ray analysis was performed in a Siemens D-5000 diffractometer with monochromatic Mo Kα radiation. The metallograph and the morphology of the mechanically alloyed powder were examined with a Hitachi S-4100 scanning electron microscope. The thermal stabilities of the amorphous powders formed were determined using a DuPont 1700 differential thermal analyser. During the thermal analysis, the sample was heated from room temperature to 1300 °C in a purified argon atmosphere.

3. Results and discussion

Fig. 1 illustrates the change in the particle size for the $Ni_{50}Ta_{50}$ powder as a function of the MA time. The size of the powder has been determined from the SEM observations as shown in the inset of Fig. 1. It is clear that the MA process for preparing $Ni_{50}Ta_{50}$ can be classified into three distinct stages: the cold-welding, the fracturing, and the steady-state stage, respectively. At the cold-welding stage (0–1 h), there is a sharp increase in the particle size due to the predominance of cold welding of Ni and Ta elemental powder. In the fracturing stage (1–5 h), the particles become harder and the fracturing of powders become dominant, resulting in a continuous decrease of particle size. During the steady-state stage (5–20 h), the balance between cold welding and fracturing of powders is achieved which leads to a relatively constant particle size. Fig. 2 shows the etched cross-section of $Ni_{50}Ta_{50}$ particles at different milling times. A typical lamellar morphology was formed after ball milling for 1 h. The individual layer thickness varied from 0.5 to 4 μm. These lamellar structures were highly refined when further milled for 5 h. After milling for 20 h, the lamellar spacings vanished, which indicated that the steady-state stage of the MA process dominated the ball-milling procedure for the period from 5 to 20 h. Fig. 3 shows the X-ray diffraction patterns of the as-milled $Ni_{50}Ta_{50}$ powders as a function of MA time. After MA for 5 h, most Bragg peaks from pure Ni have already disappeared and the intensities of the Bragg peak from Ta have decreased. The peaks of body-centred cubic (b.c.c) Ta also broadened asymmetrically towards the large-angle side because of the dissolution of the smaller Ni atoms in the b.c.c. lattice. Both the intensity decrease and the broadening of diffraction peaks are common phenomena during the early period of the MA process [10]. After ball milling for 20 h, only a broad diffraction peak exists around $2\theta = 18.7°$, which means that fully amorphous powders were formed.

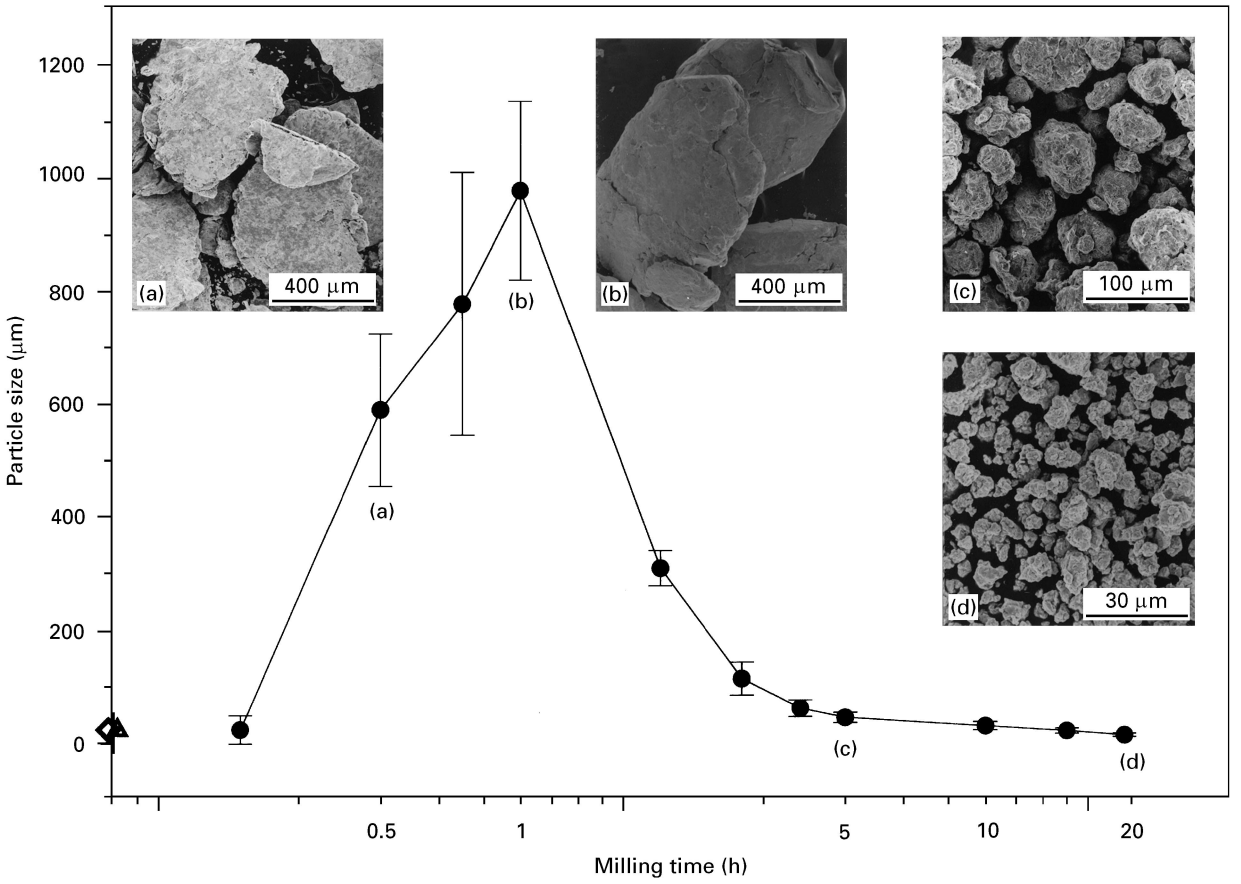

Figure 1 Particle size distribution and scanning electron micrographs (inset) for mechanically alloyed $Ni_{50}Ta_{50}$ powder after different milling periods. (◇), Ta; (△), Ni.

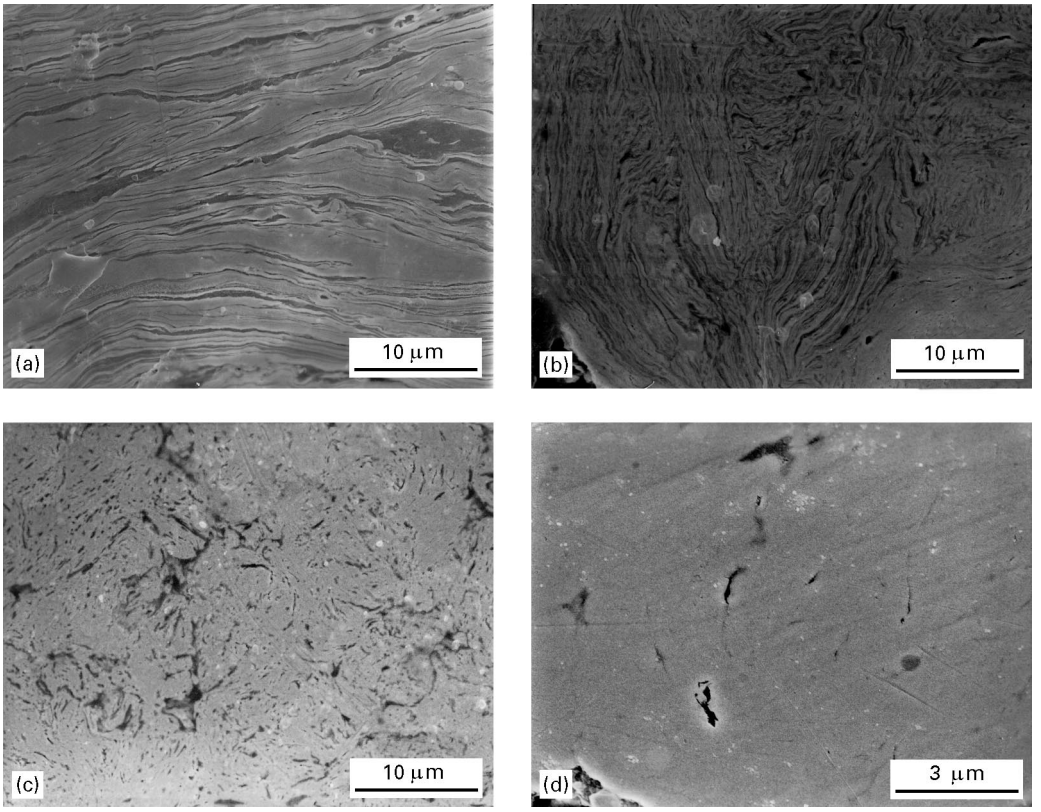

Figure 2 Microstructure of mechanically alloyed $Ni_{50}Ta_{50}$ powder particles after different milling periods: (a) 1 h; (b) 5 h; (c) 10 h; (d) 20 h.

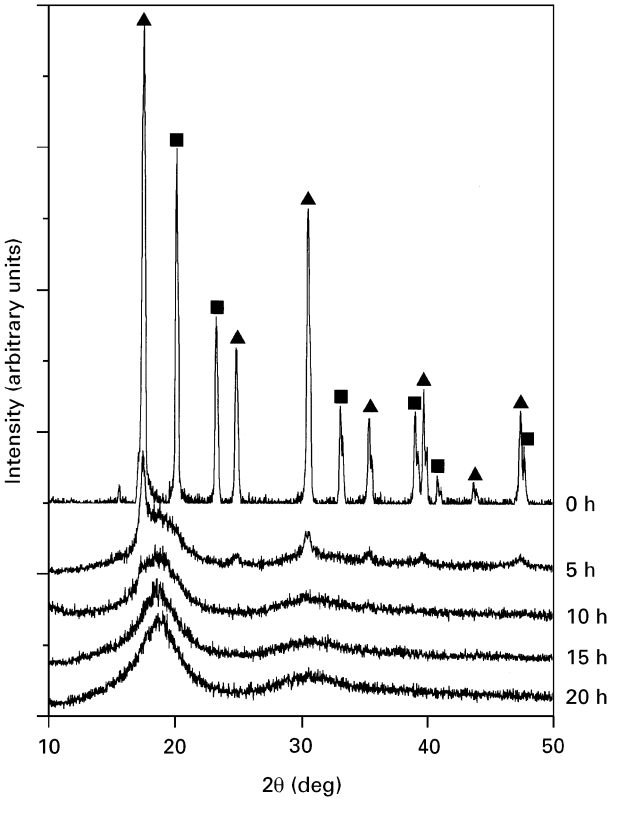

Figure 3 X-ray diffraction patterns of $Ni_{50}Ta_{50}$ as a function of milling time. (▲), Ta; (■), Ni.

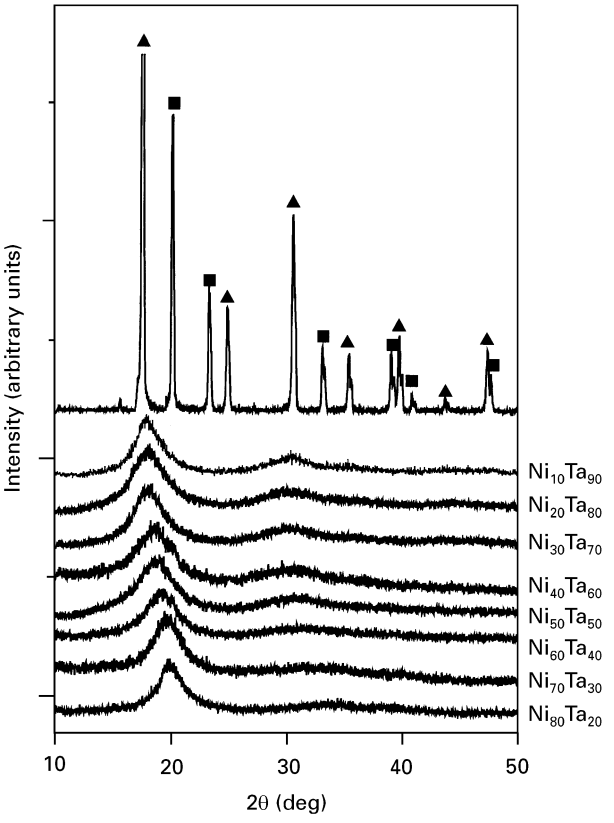

Figure 4 X-ray diffraction patterns of Ni_xTa_{100-x} powders after a MA treatment for 15–20 h. (▲), Ta; (■), Ni.

Fig. 4 shows the corresponding X-ray diffraction patterns of Ni_xTa_{100-x} alloy powders after MA treatment for 15–20 h. The powders were amorphous for the composition range between $Ni_{10}Ta_{50}$ and $Ni_{80}Ta_{20}$. This range is larger than amorphous alloys produced by the rapid-quenching process (40–70 at% Ni [11]; 35–65 at% Ni [12]; 50–70 at% Ni [13]) or by the electron-gun deposition technique (20–55 at% Ni [14]). The formation of amorphous Ni–Ta alloys at compositions containing between 10 and 30 at% Ni

has never been attained by the splat-cooling technique. The absence of eutectic and the presence of a high liquidus temperature in this composition range are presumably responsible for the inability to form an amorphous phase by rapid solidification. For $Ni_{90}Ta_{10}$, the powder is a face-centred cubic nickel-rich solid solution. The maximum solubility of nickel solid solution is found to be 17.2 at% Ta at 1360 °C [15]. The solubility at lower temperatures was much less than this value (3 at% Ta at 800 °C). Thus, the solubility limit of terminal solid solution at low temperatures in this system can be extended by the MA process. A similar extension of the primary solubility by MA has been observed in several alloy systems, for example, in Ni–Nb [16] and Cu–Ti [17].

Fig. 5 shows the corresponding X-ray diffraction patterns of Ni_xTa_{100-x} alloy powders after ball-milling treatment for 5 h. At Ni- or Ta-rich compositions ($Ni_{10}Ta_{90}$–$Ni_{30}Ta_{70}$ and $Ni_{70}Ta_{30}$–$Ni_{90}Ta_{10}$), little or no amorphous phase was found because the crystalline peaks of Ni and Ta powders still existed. However, for the composition range between $Ni_{40}Ta_{60}$ and $Ni_{60}Ta_{40}$, most Ni diffraction peaks disappeared and a broad diffraction peak was superimposed on the Ta(110) diffraction peak at around $2\theta = 18$–$20°$. This indicates that the ball-milled powders were mixtures of Ta solid solution and amorphous phases. Many researchers [10] have reported that the formation of binary amorphous alloys by MA is much easier for compositions with a large negative heat of mixing, H_m. The values of H_m as calculated by the model of Miedema *et al.* [18] show H_m to be large for Ta–(40–60) at% Ni and small for both Ni- and Ta-rich alloys. This implies that the amorphization

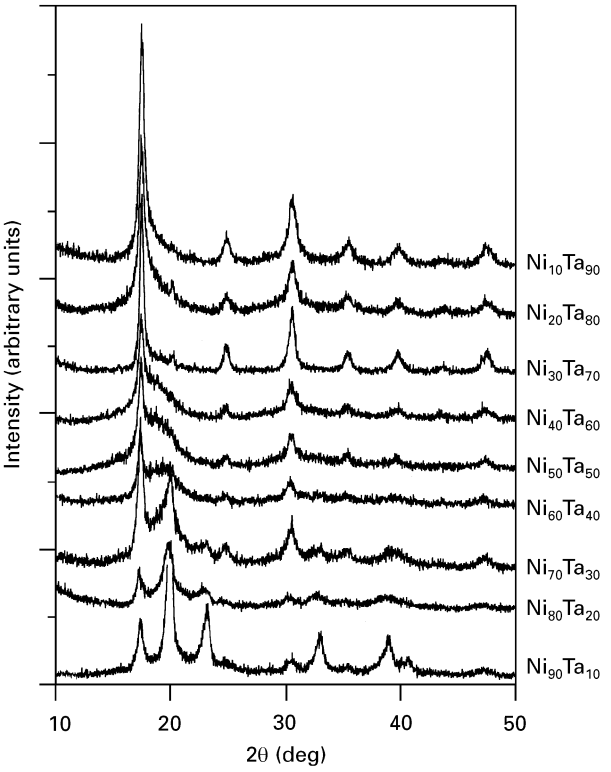

Figure 5 X-ray diffraction patterns of Ni_xTa_{100-x} powders after a MA treatment of 5 h.

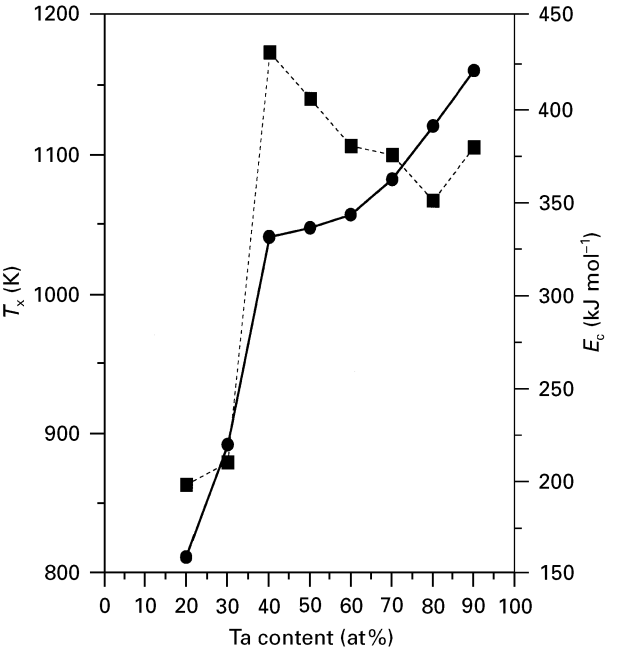

Figure 6 The crystallization temperature T_x (—●—) and activation energy E_c (– – –■– – –) of amorphous Ni–Ta powders.

rate should be faster in the intermediate compositions than those for both Ni- and Ta-rich compositions, as observed in this study.

Finally, we have investigated the stability of the Ni–Ta amorphous powders. Fig. 6 shows the crystallization temperature, T_x as a function of Ta content. The crystallization temperatures were defined from the peak position of the first peak in the DTA scans. The values of T_x corresponds to a scan rate of 40 K min^{-1}. There is a general increase in T_x as the Ta content is increased. The results of Prokoshina and Belousov [13] showed a similar crystallization temperature–Ta content dependence at compositions between 30 and 50 at% Ta for melt-spun samples, but with generally lower crystallization temperature values. For most amorphous metallic alloys, T_x is between 0.4 and 0.6 of the melting temperature [19]. This suggests that the existence of alloy compositions with a high liquidus temperature is favourable for the appearance of a high T_x. Examination of the Ni–Ta phase diagram shows that there is a general monotonic increase of liquidus temperature for high-Ta compositions. Rohr *et al.* [12] have measured T_x for their splat-quenched $Ni_{100-x}Ta_x$ ($x = 35$–60) amorphous samples by a resistivity measurement. They found that values of T_x for all samples examined were higher than 950 K. Examination of Fig. 5 shows that at the compositions between 40 and 90 at% Ta the T_x lie between 1050 and 1150 K, which is in agreement with the results of Rohr *et al.* [12] Fig. 6 also reveals the activation energy, E_c, of the Ni–Ta amorphous powders as a function of Ta content. With increasing Ta content, E_c reached a maximum at the Ni–40 at% Ta composition and then decreased rapidly. The results of previous investigations on the thermal stability of TM–Ni (TM = Fe, Hf, Ti or Zr) have indicated that a high value in activation energy is associated with a eutectic composition [20–22]. Our results were consistent with this argument as the

eutectic composition in the Ni–Ta system is Ni–36 at% Ta.

4. Conclusion

In summary, the investigations on amorphization of mechanically alloyed Ni–Ta powders were performed and results showed that complete amorphization was possible for the composition range between $Ni_{10}Ta_{90}$ and $Ni_{80}Ta_{20}$. This range is larger than amorphous alloys prepared by the splat-cooling process or by electron-gun deposition technique. A supersaturated nickel solid solution formed for Ni-rich compositions. The crystallization temperature of amorphous Ni–Ta powders was proportional to Ta content, and the activation energy of amorphous Ni–Ta powders exhibited a maximum near the eutectic composition. It is found that the amorphization rate at the early stage of the MA process is faster in the intermediate compositions and slower for both Ni- and Ta-rich compositions.

Acknowledgement

The authors are grateful for the financial support of this work by the National Science Council of the Republic of China under Grant NSC 83-0405-E-019-002.

References

1. S. DAVIS, M. FISCHER, B. C. GIESSEN and D. E. POLK, in "Rapid quenched metals III", Vol. 2, edited by B. Cantor (Metals Society, London, 1978) p. 425.
2. D. TURNBULL, *Metall. Trans. B* **12** (1981) 217.
3. X. L. YEH, K. SAMWER and W. L. JOHNSON, *Appl. Phys. Lett.* **42** (1983) 24.
4. R. B. SCHWARZ and W. L. JOHNSON, *Phys. Rev. Lett.* **51** (1983) 415.
5. W. L. JOHNSON, *Prog. Mater. Sci.* **30** (1986) 81.
6. J. S. BENJAMIN, *Sci. Amer.* **234** (1976) 40.
7. *Idem.*, *Metall. Trans.* **1** (1970) 2943.
8. C. C. KOCH, O. B. CAVIN, C. G. McKAMEY and J. O SCARBROUGH, *Appl. Phys. Lett.* **43** (1983) 1017.
9. C. C. KOCH, *Mater. Sci. Technol.* **15** (1991) 193.
10. A. W. WEEBER and H. BAKKER, *Physica B* **153** (1988) 93.
11. B. C. GIESSEN, M. MADHAVA and D. E. POLK, *Mater. Sci. Engng* **23** (1976) 145.
12. L. ROHR, P. REIMANN, T. RICHMOND and H.-J. GUNTHERODT, *Mater. Sci. Engng* **A133** (1991) 715.
13. G. F. PROKOSHINA and O. K. BELOUSOV, *Russ. Metall. Met.* **6** (1991) 170.
14. A. SCHAFER and G. MENZEL, *Thin Solid Films* **52** (1978) 11.
15. A. NASH and P. NASH, *Bull. Alloy Phase Diagram* **5** (1984) 259.
16. P. Y. LEE and C. C. KOCH, *J. Non-Cryst. Solids* **94** (1987) 88.
17. C. POLITIS and W. L. JOHNSON, *J. Appl. Phys.* **60** (1986) 1147.
18. A. R. MIEDEMA, P. F. DECHATEL and F. R. DEBOER, *Phys. B* **100** (1980) 1.
19. A. CALKA, M. MADHAVA, D. E. POLK and B. C. GIESSEN, *Scripta Metall.* **11** (1977) 65.
20. K. H. BUSCHOW, *Philips J. Res.* **39** (1984) 255.
21. Z. ALTOUNIAN, G.-H. TU and J. O. STROM-OLSEN, *J. Appl. Phys.* **53** (1983) 3111.
22. Z. ALTOUNIAN, C. A. VOLKERTAND and J. O. STROM-OLSEN, *ibid.* **57** (1985) 1777.

Received 19 April 1996
and accepted 29 July 1997